Mol Cell Biochem (2009) 325:41–51
DOI 10.1007/s11010-008-0018-9

Capillary isotachophoresis study of lipoprotein network sensitive to apolipoprotein E phenotype. 1. ApoE distribution between lipoproteins

Alexander D. Dergunov · Anne Ponthieux · Maxim V. Mel'kin · Daniel Lambert · Sophie Visvikis-Siest · Gerard Siest

Received: 28 August 2008 / Accepted: 30 December 2008 / Published online: 13 January 2009

Abstract Sixteen patients differing widely in plasma triglyceride content were divided into three groups by their apolipoprotein E (apoE) phenotype—E33 homozygotes, E23, and E34 heterozygotes. The plasma lipid and apoE distribution between individual lipoproteins was followed by capillary isotachophoresis (CITP) of plasma samples prestained with lipid fluorescent probe NBD-C6-ceramide and by fluorescein-labeled apoE, respectively. Among 12 peaks visualized by ceramide staining, an individual peak with very low density lipoproteins (VLDL) was identified. The VLDL cholesterol and apoE content determined by CITP directly in whole plasma were significantly related to their content as determined by conventional analysis with isolated VLDL. The ceramide distribution among lipoprotein pools was insensitive to apoE phenotype (49–53 : 7–11 : 39–43% for HDL, VLDL, and IDL/LDL, respectively) while the preferential binding of apoE to VLDL was observed in E34 patients compared to E33 (62 : 19 : 20 vs. 70 : 9 : 22%). In a study of apoE/F displacement from lipoproteins at plasma titration by apoC-III in vitro, apoE was found to bind more tightly to VLDL from E34 compared to E33 patients as evidenced by both the increased non-displaceable apoE pool, the increased VLDL sorbtion capacity for apoE, and the decreased displacement parameter in a "container" model of lipoprotein binding. Two different types of apoE package in a whole lipoprotein profile were observed. ApoE structure in a particular lipoprotein may underlie the phenotype-sensitive apoE distribution and apoC-III interference in hypertriglyceridemia.

Keywords Apolipoprotein C-III · Apolipoprotein E · Capillary isotachophoresis · Hypertriglyceridemia · Lipoprotein binding · Metabolic network

A. D. Dergunov (✉) · M. V. Mel'kin
National Research Centre for Preventive Medicine,
10, Petroverigsky street, 101990 Moscow, Russia
e-mail: dergunov@img.ras.ru

A. Ponthieux · D. Lambert · S. Visvikis-Siest · G. Siest
Faculte de Pharmacie, INSERM U525 - Equipe 4,
EA 4003, Université Henri Poincaré, 30 rue Lionnois,
54000 Nancy, France

Introduction

Hypertriglyceridemia is an independent risk factor for cardiovascular disease [1] and is characterized by elevated levels of very low density lipoproteins (VLDL), is often associated with low levels of high density lipoproteins (HDL), the accumulation of small dense low density lipoproteins (LDL), and insulin resistance. Both overproduction and delayed clearance of VLDL have been demonstrated in hypertriglyceridemia [2]. Apolipoprotein E (apoE) is involved in the hepatic uptake of lipoprotein particles, lipolysis of triglyceride(TG)-rich lipoproteins, and stimulation of cholesterol (Ch) efflux from macrophage foam cells in atherosclerotic lesions. At the same time, apoE within hypertriglyceridemic triglyceride-rich lipoproteins is thought to be a ligand for macrophage receptor(s) promoting foam cell formation [3]. Besides the direct interaction of apoE with receptors and lipases [3–5], the efficient clearance and lipolysis of TG-rich lipoproteins may be modulated by changes in apoE content and/or distribution mediated by apoC-III. However, this process still remains controversial and poorly understood [6–8]. In humans, apoE is polymorphic, and this genetic variation has a strong effect

on its atherogenic-related characteristics. The three isoforms of apoE differ by single amino acid changes. In comparison with ε3 (corresponds to apoE3 isoform C112-R158), the ε4 allele (apoE4 isoform R112-R158) is associated with clinical and coronary disease [9] while ε2 allele (apoE2 isoform C112-C158) seems to be associated with lower Ch levels. ApoE normally self associates in solution and consists of two N- and C-terminal domains [10–12]. The apoE folding pathway includes one [13, 14] or more [15] intermediate form(s), populated differently among the three isoforms and important in lipid binding. In normolipidemics, the majority of plasma apoE is transported on HDL [16, 17]. A number of HDL particles that contain apoE, but not apoA-I, have been identified in plasma [18–21]. These HDL particles exhibit either γ-, preβ-, or α- electrophoretic mobility.

Among the various approaches used to separate plasma lipoproteins, capillary isotachophoresis (CITP) has become one of the most powerful techniques [22–27] due to high speed and efficiency, and a single run separation of different lipoproteins. However, the wide use of CITP is limited by the lack of a standard description of the localization and identification of particular lipoproteins within separation profile. For instance, the exact location of preβ-HDL in the CITP profile [26] and the estimate of its relative content among total HDL [28] are not yet confirmed. The existing methods for plasma apoE separation into lipoprotein-bound pools, including ultracentrifugation [29, 30], gel chromatography [16, 17, 31–34], and other approaches [20, 35, 36] with subsequent apoE detection in fractions obtained, generally suffer from low resolution and are both labor- and time-consuming. Moreover, a 10-fold discrepancy exists between the estimates of apoE content in VLDL particles, i.e., 2–4 [37] vs. 18–41 [38] apoE molecules/particle.

Currently, there have been no attempts to combine the high-CITP separation efficiency with an apoE-specific detection system. The aim of the present study was therefore (i) to develop a CITP-based approach to concurrently detect lipid and apoE distribution among lipoproteins in whole plasma from patients with three major apoE isoforms, who differ widely in plasma TG content; (ii) to accurately locate VLDL particles in the CITP profile; and (iii) to quantitatively describe the underlying mechanism of apoE distribution revealing the competition of apoE and other exchangeable apolipoprotein, apoC-III, at lipoprotein binding. In an adjacent paper in this issue, this approach was used to visualize the metabolic links between different apoE compartments both at stationary and lipolysis-stimulated conditions.

Materials and methods

Subjects and blood sampling

Ambulatory patients occasionally visiting the National Research Centre for Preventive Medicine in Moscow were recruited. Both male and female subjects in a wide-age range were included; the local ethical committee approval was received and the informed consent of all participating subjects was obtained. Patients were selected if they had not been taking lipid-lowering medications for at least one month before the study. They were excluded if they had had a myocardial infarction or unstable angina. The patients were divided into three groups on the basis of their apoE phenotypes. The first group included only E33 homozygotes (E33 group). The second group contained E23 heterozygotes (E23 group). The third group contained E34 heterozygotes (E34 group). The plasma lipid and apolipoprotein values and group composition are shown in Table 1. In order to stimulate lipolysis in vivo, heparin (50 IU/kg) was injected intravenously and venous blood samples were obtained from the patients both before and 10 min after heparin injection. Blood was collected on EDTA, put immediately on ice and plasma was separated by centrifugation at 2500 rpm for 10 min at 4°C. Phenylmethanesulfonyl fluoride (PMSF) was added to plasma to a final concentration of 1 mM to inhibit both lipoprotein lipase [39] and LCAT [40] activities. The lipoprotein isolation was started within 4 h after plasma separation.

Lipoprotein isolation

Very low density lipoproteins ($d < 1.006$ g/cm^3) were isolated from plasma by sequential ultracentrifugation [41]. PMSF was added to 0.4 mM to the density solution.

Apolipoprotein isolation and labeling

ApoE [42] and apoC-III-1 [43] were isolated as described. The purity of the apolipoproteins measured by 5–20% SDS-PAGE and additionally for apoC-III-1 by urea-PAGE was greater than 95%. The reduction of disulfide bonds and blockage of thiol groups of apoE by iodoacetamide (alkylation) was performed [44]. Native or alkylated apoE (5.6 μM) was labeled with fluorescein isothiocyanate (Isomer 1, Sigma, St.Louis, Missouri, USA) in 0.1 M $NaHCO_3$, pH 9.2 at a dye/protein molar ratio around 10:1. Extent of labeling was varied by varying the incubation times, which never exceeded 14 h. Unreacted dye was separated by gel-filtration on a PD-10 column (Pharmacia/LKB, Uppsala, Sweden) equilibrated with 0.02 M

Table 1 Antropometric, plasma lipid and apolipoprotein values and composition of isolated VLDL particles in patient groups divided by apoE phenotype before and 10 min after intravenous administration of heparin (50 IU/kg)

		E33		E23		E34	
		Before	After	Before	After	Before	After
	Age, years	41.5 ± 3.2		46.0 ± 4.0		54.8 ± 3.3	
	BMI, kg/m^2	29.86 ± 1.96		30.4 ± 8.2		26.83 ± 0.60	
	Sex, male(M)/female (F)	5 M/5 F		2 M/0 F		4 M/0 F	
Plasma	TG, mM	2.00 ± 0.27	1.62 ± 0.25**	2.95 ± 1.35	2.26 ± 0.94	3.34 ± 0.70	2.92 ± 0.62*
	Ch, mM	5.46 ± 0.32	5.12 ± 0.24	4.95 ± 0.33	4.19 ± 0.05$^{2–4,}$ *	6.23 ± 0.48	5.98 ± 0.37
	LDL-Ch, mM	3.47 ± 0.30	3.29 ± 0.23	2.59 ± 0.07	2.21 ± 0.25	4.00 ± 0.31	3.72 ± 0.40
	HDL-Ch, mM	1.09 ± 0.07	1.10 ± 0.07	1.03 ± 0.21	0.96 ± 0.13	0.97 ± 0.15	0.94 ± 0.11
	ApoA-I, g/l	1.26 ± 0.11	1.34 ± 0.07	1.43 ± 0.08	1.39 ± 0.12	1.14 ± 0.08	1.11 ± 0.08
	ApoB, g/l	1.00 ± 0.09	1.06 ± 0.06	0.83 ± 0.14	0.84 ± 0.12$^{2–4,}$ *	1.29 ± 0.08	1.25 ± 0.08
	ApoE, mg/l	43.64 ± 3.06	41.38 ± 2.38	59.78 ± 8.95	69.59 ± 18.02$^{2–3,}$ *	51.67 ± 6.01	50.62 ± 4.50
	ApoC-III, mg/l	104.77 ± 12.17	99.23 ± 10.92	135.54 ± 28.94	134.66 ± 33.02	133.01 ± 19.43	127.47 ± 16.57
VLDL	TG/apoB molar ratio	6679 ± 569	5114 ± 672**	8694 ± 2365	5905 ± 1672	7693 ± 1075	5484 ± 775**
	Ch/apoB molar ratio	2344 ± 197$^{3–4,}$*	2507 ± 181	2999 ± 476	2925 ± 544	3402 ± 399	3214 ± 355
	ApoE/apoB molar ratio	2.12 ± 0.12	1.89 ± 0.29	2.71 ± 0.60	2.23 ± 0.71	2.62 ± 0.34	1.92 ± 0.16
	ApoC-III/apoB molar ratio	26.24 ± 3.84	16.03 ± 3.66	34.49 ± 8.47	16.99 ± 5.46	30.24 ± 2.69	13.61 ± 3.34**

The superscripts denote the significant differences at "before" vs. "after" comparison within a group with particular apoE phenotype: * $P < 0.05$, ** $P < 0.01$

$^{2–3}$ E23 vs. E33 comparison of identical ("before" or "after") sub-groups

$^{2–4}$ E23 vs. E34 comparison of identical ("before" or "after") sub-groups

$^{3–4}$ E33 vs. E34 comparison of identical ("before" or "after") sub-groups

tris–HCl, pH 7.5, 0.15 M NaCl, 0.1 mM EDTA and by subsequent dialysis against a 100-fold excess of the buffer. In the case of native apoE, 1 mM dithiothreitol was added. Samples were filtered through a 0.45 μ filter and the protein concentration in the labeled samples was determined [45] with native or alkylated apoE as a standard based on a molar extinction coefficient of $\varepsilon_{280} = 43\ 376\ M^{-1}\ cm^{-1}$. The labeling stoichiometry was calculated using $\varepsilon_{495} = 42\ 500\ M^{-1}\ cm^{-1}$ for bound fluorescein [46].

Capillary isotachophoresis

Plasma staining with lipophilic fluorescent probe NBD-C6-ceramide (Molecular Probes, Eugene, OR, USA) and separation conditions were described elsewhere [24, 25, 47]. Briefly, 5 µl of plasma was diluted with 5 µl of water, 5 µl of 1 mg/ml ceramide solution in DMSO/ethylene glycol (1:9 v/v, dye solvent) was added and after 10 min of incubation, 25 µl of spacer mixture was added. The stock solution of spacers was prepared by mixing of 50 µl of each spacer solution at 10 mg/ml and contained *N*-tris[hydroxymethyl]methylglycine, *N*-tris(hydroxymethyl)methyl-2-aminoethanesulfonic acid, L-glutamine, L-serine, D-glucuronic acid, 1-octanesulfonic acid (Na salt), L-methionine, *N*-[2-acetamido]-2-aminoethanesulfonic acid, glycine (25 µl), *N*-tris[hydroxymethyl]methyl-3-aminopropanesulfonic acid (75 µl). 25 µl of 5-carboxyfluorescein as an internal marker was added to the 500 µl of the stock solution and 100 µl was diluted with 500 µl of the leading buffer. A few nanoliters of sample were injected by pressure in a coated fused silica capillary. The separation was performed on a P/ACE system 5510 (Beckman Coulter, Fullerton, CA, USA) equipped with an argon laser-induced fluorescence detector with excitation at 488 nm and emission at 520 nm. For apoE staining, 0.5 µl of 7.79 µM fluorescein-labeled apoE (apoE/F) at labeling stoichiometry as 3.6 mole of fluorescein/mole of protein were added to 20 µl of plasma, diluted with 29.5 µl of P_i buffer (10 mM P_i/Na, pH 7.4, 0.15 M NaCl, 0.01% NaN_3) followed by the incubation for 90 min at 37°C and overnight at 4°C. For CITP separation, the apoE/F-prestained samples were then treated as ceramide-stained aliquots with dye solvent substituting for probe solution. To localize VLDL peak(s) within the CITP profile, the surplus of autologous VLDL was added to plasma sample and the aliquots were proceeded with ceramide and apoE/F staining as above. The elution profiles were deconvoluted into individual Gauss-shaped components with PeakFit Version

4.12 (SeaSolve Software Inc., Framingham, MA, USA) by the second derivative routine. Both absolute (APA) normalized to internal standard and relative peak areas (RPA) were used in the data treatment (Eq. 1):

$$\mathrm{RPA}_i = \frac{\mathrm{APA}_i}{\sum_i \mathrm{APA}_i} \quad (1)$$

Total plasma Ch and apoE content and the respective relative peak areas in ceramide and apoE profiles were used to calculate Ch (Eq. 2) and apoE (Eq. 3) content within VLDL (peaks 8C and 8E, respectively):

$$\mathrm{VLDL-Ch(mM)} = \mathrm{RPA(8C)} \cdot \mathrm{Ch_{plasma}(mM)} \quad (2)$$

$$\mathrm{VLDL-apoE(mg/L)} = \mathrm{RPA(8E)} \cdot \mathrm{apoE_{plasma}(mg/L)} \quad (3)$$

Displacement study

The relative affinity of apoE to lipoproteins in whole plasma was estimated from the displacement of lipoprotein-bound apoE/F by exogenous apoC-III-1. The 50 µl of reaction mixture in phosphate buffer contained 20 µl plasma, 77.5 nM apoE/F (9.6–23.8% of plasma apoE), and 1, 2, 3, and 5 µl of apoC-III-1 stock solution at concentation 225 µM. At the final titration point, the total apoC-III quantity 3.9–8.7 fold exceeded the endogenous apolipoprotein for 16 patients. The samples were incubated for 90 min at 37°C and overnight at 4°C and the residual apoE/F content in lipoproteins was analyzed by CITP as above. To construct the titration curve, several apoE/F and a single ceramide profiles are to be measured. The data were treated within a "container" model with lipoproteins as independent containers for exchangeable apolipoproteins. In this model, at titration point i the original and residual apoE levels in a particular lipoprotein j are determined by a product of apoE original content and the ratio of residual and original signals from fluorescein-labeled apoE (Eq. 4), while apoC-III content in this lipoprotein is determined by the relative size of lipoprotein surface that is assumed to be reported by ceramide probe distribution measured in parallel (Eq. 5). The decrease of apoE/F signal at plasma titration by apoC-III is modeled by exponential decay (Eq. 6):

$$\mathrm{E}_j^i(\mathrm{nM}) = \frac{\mathrm{APA}_j^i}{\mathrm{APA}_j^0} \cdot \mathrm{RPA(E)}_j \cdot \mathrm{E_{plasma}(nM)} \quad (4)$$

$$C-\mathrm{III}_j^i(\mathrm{nM}) = \left(C-\mathrm{III_{plasma}} + C-\mathrm{III}_{\mathrm{added}}^i\right) \cdot \mathrm{RPA(Cer)}_j \quad (5)$$

$$\mathrm{E}_j^i(\mathrm{nM}) = A_1 + A_2 \cdot e^{-A_3 \cdot C-\mathrm{III}_j^i(\mathrm{nM})} \quad (6)$$

The A_1 parameter corresponds to the size of apoE non-displaceable pool; the A_2 parameter corresponds to the maximal sorbtion capacity for apoE of the particular "container" without any interference by apoC-III and/or other amphipathic apolipoproteins; the A_3 parameter is related to the relative affinity and decreases at affinity increase.

Analytical methods

Cholesterol and triglyceride content in plasma and isolated lipoproteins were determined using standard enzymatic methods, CHOD-PAP and GPO-PAP, respectively. HDL-Ch was determined after precipitation of apoB-containing lipoproteins with phosphotungstic acid/$MgCl_2$ [48]. LDL-Ch was calculated using the Friedewald formula [49]. ApoE and apoC-III were quantified by turbidimetry and apoB and apoA-I by nephelometry both in plasma and VLDLs using Cobas–Mira autoanalyzer (Roche Diagnostic Systems, Neuilly sur Seine, France) and Behring nephelometer (Rueil-Malmaison, France), respectively. The apoE genotype was determined by restriction isotyping [50]. The number of TG, Ch, apoE, and apoC-III molecules within VLDL particles was estimated based on a stoichiometry of one $\mathrm{apoB_{100}}$ molecule per particle.

Statistical methods

The statistical comparisons of clinical and biochemical parameters were performed with STATISTICA version 6 (StatSoft, Inc. (2001) Tulsa, OK, USA). Results are expressed as mean ± SEM. The variables were $\log_{10}$ transformed before the analyses, but the values in text, tables, and figures are presented as non-transformed. The variables were compared between the groups by a general linear model, analysis of variance (ANOVA) or analysis of covariance (ANCOVA). $P < 0.05$ was considered significant. Tree-clustering analysis was used to compare the apoE package between lipoproteins.

Results

Patient groups by apoE phenotype

Three patient groups formed by apoE phenotype—homozygotes E33, heterozygotes E23, and E34—did not differ from each other by anthropometric and basal, i.e., before heparin administration ("before" values), plasma lipid ($\mathrm{TG_b}$, $\mathrm{Ch_b}$, HDL-$\mathrm{Ch_b}$ and LDL-$\mathrm{Ch_b}$), and apolipoprotein ($\mathrm{apoA\text{-}I_b}$, $\mathrm{apoB_b}$, $\mathrm{apoE_b}$ and $\mathrm{apoC\text{-}III_b}$) values (Table 1). The VLDL particles isolated from E34 patients contained more cholesterol, based on one apoB molecule per particle stoichiometry. ApoE content varied as 2.12–2.71 apoE

molecules/particle depending the phenotype. The VLDL partiles contained at a mean level 48%, 60%, and 56% of plasma triglyceride for E33, E23, and E34 groups, respectively. To stimulate lipolysis in vivo, heparin at 50 IU/kg was injected and 10 min after the plasma samples were withdrawn ("after" values). The plasma triglyceride TG_a decreased in all three groups by 21%, 21%, and 12% at a mean level for E33, E23, and E34 groups, respectively. This decrease was statistically significant for E33 and E34 groups. The cholesterol content in post-lipolytic plasmas from E23 patients was significantly lower compared to E34 patients in accordance with isoform effect on Ch level in the general population. The plasma $apoB_a$ content changed analogously. In contrast, the plasma $apoE_a$ content in E23 group was the highest, compared to E33 group. The plasma apoA-I_a and apoC-III_a content did not differ significantly between the three groups. The triglyceride content in VLDL particles isolated from post-lipolysis plasma aliquots, decreased by 38%, 40%, and 43% for E33, E23, and E34 groups, respectively. This decrease was significant for E33 and E34 groups. The apoE content in post-lipolysis VLDL (1.89–2.23 apoE molecules/particle) tended to decrease, although not significantly. Analogously, the apoC-III_a content (13.6–17.0 apoC-III molecules/particle) decreased, being significant for the E34 group.

The localization of VLDL particles in ceramide- and apoE-specific lipoprotein profiles by CITP

Up to 12 components were detected in the profiles at the conventional pre-staining of plasma aliquots before heparin administration by lipid-specific probe (the fluorescent ceramide analog), and the subsequent lipoprotein separation by CITP (Fig. 1). To visualize apoE distribution among plasma lipoproteins, the fluorescein-labeled apoE was added to plasma aliquots at the indicator quantities to minimize the perturbing action of apoE/F on the distribution of endogenous apoE. Up to 11 components were detected by apoE/F staining and subsequent lipoprotein separation by CITP at the same conditions as for ceramide-stained samples (Fig. 1).

To identify VLDL particles in a total profile the surplus quantities of the autologous VLDL were added to plasma and the additional separations with two pre-staining types were performed. At VLDL addition, selective increase in the area of the eighth peak in both ceramide- ($8C_b$) and apoE-profiles ($8E_b$) was observed (Fig. 1) evidencing the isolated VLDL peak. The decrease of some components other than the $8E_b$ in apoE-profile at the VLDL abundance is reasonable due to the apoE/F deficiency relative to lipoprotein binding sites, in contrast to the excess in

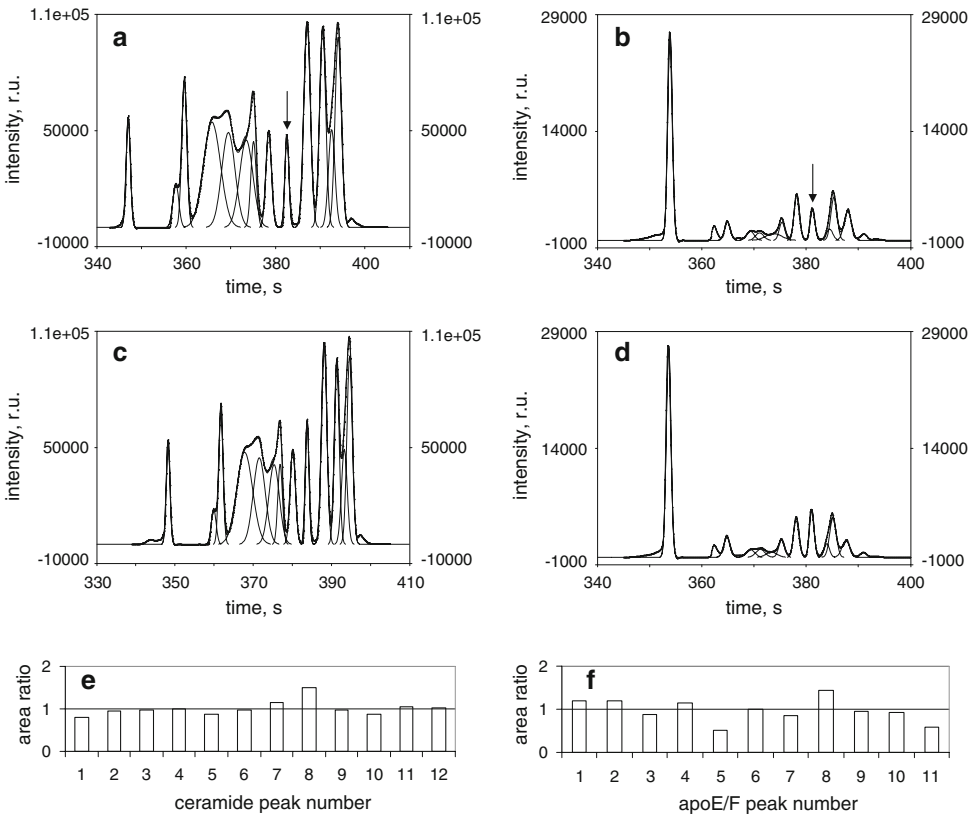

Fig. 1 The location of VLDL in CITP profile of patient 13 detected by ceramide and apoE/F before heparin administration. The ceramide (**a**, **c**, **e**) or apoE/F (**b**, **d**, **f**) profiles were obtained before (**a**, **b**) or after (**c**, **d**) addition of autologous VLDL and the changes in peak area for ceramide and apoE/F staining are given (**e**, **f**). The location of VLDLs in the profiles are indicated by arrows. Plasma TG = 1.32 mM, HDL-Ch = 1.27 mM, E34 phenotype

ceramide quantities. Thus, the accurate identification of VLDL particles with preβ-mobility in the center of the profile permits the location of both faster HDL particles with α- and preβ-mobility and slower IDL/LDL particles with β-mobility. A similar lipoprotein location in CITP profile under analogous electrophoretic conditions was suggested by others [25, 26]. Based on the present and previous [24] findings, the first seven peaks in ceramide (1–7C_b) and apoE-profiles (1–7E_b) correspond to high density lipoproteins (HDL), the 8C_b and 8E_b peaks to VLDL particles and the last four peaks in ceramide- (9–12C_b) and three peaks in apoE-profiles (9–11E_b) to intermediate/low density lipoproteins (IDL/LDL). The location of the individual peaks for different plasma samples varied. In order to standardize the peak location, the relative positions of the individual peaks within both profile types were estimated (Fig. 2). The Ch and apoE content in VLDL particles estimated from relative peak areas (8C_b and 8E_b) in both profile types and plasma Ch and apoE content, significantly correlated to Ch ($r = 0.72$, $P = 0.002$) and apoE ($r = 0.88$, $P < 0.0001$) content in isolated VLDL measured by the conventional analytical methods. The 8E_b/8C_b peak area ratio at two stainings remained constant in a wide range of apoE/Ch ratio in isolated VLDL ($r = -0.032$, $P = 0.905$) proving the validity of the VLDL peak identification, its originality in lipoprotein profile (i.e., the absence of other component in this peak), and the constancy of quantum yields of two fluorescent labels in the particular lipoprotein. Thus, the Ch and apoE content in a particular lipoprotein component visualized by CITP after pre-staining of whole plasma by ceramide and apoE/F may be quantitatively measured.

ApoE phenotype-dependent lipoprotein distribution at two types of staining

The distribution of fluorescence intensity among individual lipoproteins in plasma pre-stained by ceramide probe or apoE/F was studied in three patient groups before heparin administration (Fig. 3a, b). The data on lipoprotein pools HDL, VLDL, and IDL/LDL are given in Table 2.

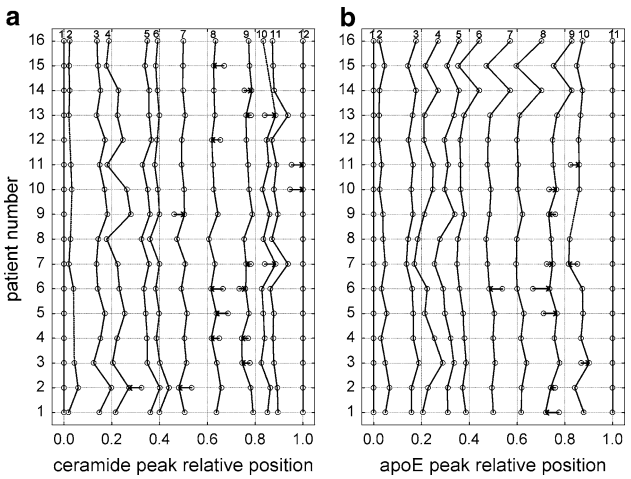

Fig. 2 The relative position of lipoprotein components in CITP profile detected by ceramide (**a**) and apoE/F (**b**). The relative position is defined as a ratio of the difference in the output time of a peak of interest and the slowest one to the difference in the output time of the slowest and fastest peaks. Generally, 12 and 11 components were present in ceramide- and apoE/F-stained profiles, respectively. The additional peak(s) evidenced in some profiles by the second derivative routine were combined with the mostly overlapping neighbor (directed by *arrows*) for subsequent analysis in terms of unifying network topology

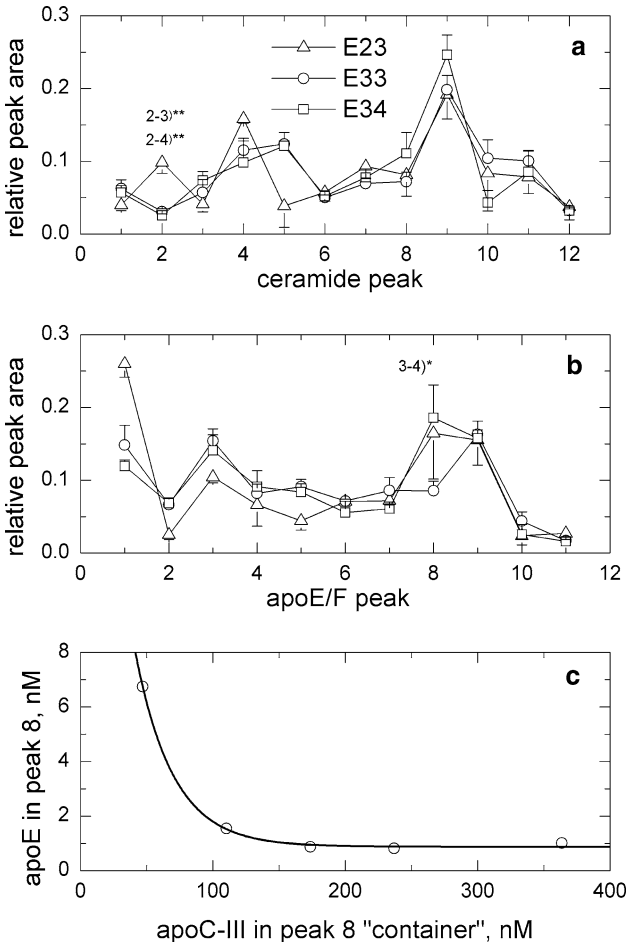

Fig. 3 The phenotype-dependent relative distribution of ceramide and apoE staining and relative affinity of apoE in lipoprotein profile. (**a**) The comparisons were made by ANOVA between phenotypes for a particular peak: $^{2-3}$ and $^{2-4}$ differ significantly ($^*P < 0.05$, $^{**}P < 0.01$) at E23 vs. E33 and E23 vs. E34, respectively; (**b**) $^{3-4}$ differ at E33 vs E34 by ANOVA; (**c**) the displacement of apoE/F from VLDL peak at the apoC-III addition to a whole plasma of patient 8 with E33 phenotype. Data were treated within a "container" model and fitted to the equation: $y = A_1 + A_2 \times \exp(-A_3 \times x)$ with $A_1 = 0.88 \pm 0.08$ nM, $A_2 = 30.2 \pm 4.88$ nM, $A_3 = (34.9 \pm 3.5) \times 10^6$ M^{-1}

Table 2 The distribution of Cer and apoE between lipoprotein pools for three phenotype groups. The relative peak areas (mean ± SEM) of the peak(s) specified are given

	E33	E23	E34
Ceramide staining, RPA			
1–7C_b	0.50 ± 0.02	0.53 ± 0.05	0.49 ± 0.04
8C_b	0.07 ± 0.01	0.08 ± 0.03	0.11 ± 0.03
9–12C_b	0.43 ± 0.02	0.39 ± 0.02	0.40 ± 0.02
apoE/F staining, RPA			
1–7E_b	0.70 ± 0.03	0.64 ± 0.03	0.62 ± 0.03
8E_b	0.09 ± 0.01[3–4]	0.16 ± 0.06	0.19 ± 0.05
9–11E_b	0.22 ± 0.02	0.19 ± 0.03	0.20 ± 0.03
apoE/ceramide standardized area ratio			
1–7E_b/1–7C_b	0.96 ± 0.20	0.98 ± 0.003	1.61 ± 0.43
8E_b/8C_b	1.21 ± 0.49	1.61 ± 0.05	2.04 ± 0.40
9–11E_b/9–12C_b	0.36 ± 0.08	0.41 ± 0.11	0.61 ± 0.16

Ceramide staining: no significant differences between phenotypes by ANOVA

ApoE/F staining: [3–4] E33 vs. E34 comparison ($P < 0.05$ by ANOVA)

ApoE/Cer area ratio: no significant differences between phenotypes by ANOVA

At ceramide pre-staining, the major portion of the signal among E33 and E34 groups originated from the 9C_b peak that includes IDL/LDL particles and from 4C_b and 5C_b peaks that include HDL particles. The 2C_b peak possessed significantly higher fluorescence for E23 group compared to two others. After comparison of the signal distribution among lipoprotein pools the three groups did not differ from each other and generally 49–53% and 39–43% of the fluorescence originated from HDL and IDL/LDL, respectively.

The apoE/F pre-staining was phenotype sensitive, with the major portion of the signal originating from the zone of "fast" HDL (1E_b, 3E_b) and also from 9E_b (E33 group) or 8E_b (E34 group) peaks (Fig. 3b). The decrease of apoE content in VLDL from E33 homozygotes compared to E34 heterozygotes was significant. Comparing the apoE/F fluorescence distribution among lipoprotein pools, 62–70%, 9–19%, and 19–22% of the signal originated from HDL, VLDL, and IDL/LDL, respectively (Table 2). So, apoE binding to VLDL was phenotype dependent and maximal for E34 group.

Displacement study

The apoC-III influence on apoE lipoprotein content was examined by studying the efficiency of the displacement of apoE/F from a particular lipoprotein at in vitro titration of whole plasma by apoC-III. The representative data for apoE displacement from VLDL in plasma from patient 8 with E33 phenotype treated within a "container" model, are given in Fig. 3c. The whole data set for all 11 lipoprotein components among the three patient groups are given in Table 3. The detailed description of this model is given in the section "Materials and methods." The size of non-displaceable pool (A_1 parameter) in VLDL for E34 group was the highest, being significant when compared to E33 group. The A_1 parameter did not change within lipoprotein profiles for both E33 and E34 groups, although a tendency toward higher values for 3E_b and 7E_b components was observed; within E23 group, the A_1 values were significantly higher for 7E_b and 8E_b compared to 10E_b.

The maximal sorbtion capacity of a particular lipoprotein for apoE without any interference by apoC-III (A_2 parameter) was significantly higher for 1E_b in E34 group when compared to E33, with a similar tendency, although insignificant ($P = 0.13$) for 8E_b. The A_2 value for 7E_b was significantly higher in E23 group compared to E33. There were no differences in A_2 values within lipoprotein profiles for each group. It should be pointed out that the cumulative A_2 value (6.8 μM at a mean level) for all lipoproteins in the E33 group is 3–7-fold higher than the real apoE content in plasma,.i.e., apoE content is controlled by apoC-III and/or other apolipoproteins.

The efficiency of apoE displacement by apoC-III, characterized by the A_3 parameter, tended to be lower for both 8E_b and 9E_b in E34 group when compared to E33 ($P = 0.09$). The opposite tendency was observed with higher A_3 values for HDL particles in 1E_b, 2E_b, 4E_b, and 5E_b peaks. Within profiles in both E33 and E34 groups, the 2E_b component possessed the maximal A_3 value. This A_3 value did not differ from A_3 value for 8E_b in E33 group, although 3.7-fold higher at analogous comparison in E34 group. Thus, the significantly larger size of non-displaceable pool in VLDL for E34 compared to E33 group, together with tendencies to higher sorbtion capacity and a lower displacement parameter, may be associated with preferential apoE binding to VLDL in E34 compared to E33 patients.

The apoE content in a particular lipoprotein(s) may be associated with the binding efficiency predicted by the parameters of the "container" model. Indeed, for the E33 group apoE content was directly related with the size of non-displaceable pool (9E_b) and the maximal sorbtion capacity (2E_b, 5E_b, 8E_b), whereas it is inversely related to the displacement parameter (1E_b) (Table 4). For other lipoproteins, apoE content may be controlled by factor(s) other than apoC-III content.

The composition and the structure of individual lipoproteins were characterized by the ratio of absolute peak areas at apoE/F and ceramide staining as a value sensitive to both the quantum yield and/or the content of two labels (Fig. 4). Within the profile, the third peak possessed the maximal value of this ratio by both the analysis of variance

Table 3 The displacement of apoE/F from CITP lipoprotein fractions at the titration of apoE/F-stained whole plasma by apoC-III

	A_1 (nM)			A_2 (μM)			A_3 (10^6 M^{-1})		
	E33	E23	E34	E33	E23	E34	E33	E23	E34
$1E_b$	2.67 ± 1.23	n.d.	2.30 ± 0.39	0.81 ± 0.58$^{3-4}$	n.d.	29.5 ± 16.4	8.4 ± 2.1	n.d.	10.2 ± 1.0 {9}
$2E_b$	2.05 ± 0.76	1.00 ± 0.16 {7}	1.25 ± 0.32	0.77 ± 0.41	0.42 ± 0.22	0.84 ± 0.68	14.5 ± 2.4 {9}, {10}	3.46 ± 0.07$^{2-3,\ 2-4}$	18.7 ± 1.6 {9}
$3E_b$	4.28 ± 1.08	n.d.	2.85 ± 0.73	1.32 ± 0.68	n.d.	1.13 ± 0.54	10.5 ± 1.9	n.d.	5.7 ± 1.4
$4E_b$	2.80 ± 1.09	n.d.	1.92 ± 0.41	1.21 ± 0.73	n.d.	1.38 ± 1.06	4.2 ± 1.0	n.d.	7.8 ± 3.4
$5E_b$	1.95 ± 0.73	n.d.	1.63 ± 0.22	0.49 ± 0.23	n.d.	3.34 ± 1.94	3.7 ± 0.4	n.d.	4.7 ± 1.0
$6E_b$	3.29 ± 0.76	2.23 ± 0.10	3.51 ± 0.62	0.91 ± 0.73	0.66 ± 0.17	0.94 ± 0.61	8.2 ± 1.1	4.9 ± 0.4	8.6 ± 2.8
$7E_b$	8.10 ± 2.00	9.07 ± 0.00 {10}	n.d.	0.12 ± 0.04	0.38 ± 0.12$^{2-3}$	n.d.	4.1 ± 0.4	6.7 ± 3.8	n.d.
$8E_b$	4.06 ± 0.96$^{3-4}$	5.23 ± 0.05 {10}	8.60 ± 1.87	0.28 ± 0.12	3.39 ± 2.89	4.81 ± 3.85	12.1 ± 4.5	3.6 ± 0.7	5.0 ± 1.8
$9E_b$	5.99 ± 1.98	2.70 ± 0.91	3.30 ± 0.80	0.72 ± 0.31	3.01 ± 1.59	2.76 ± 2.04	2.9 ± 0.7	2.5 ± 0.2	1.50 ± 0.19
$10E_b$	1.16 ± 0.39	0.62 ± 0.17	2.01 ± 1.03	0.14 ± 0.06	0.80 ± 0.57	0.52 ± 0.44	2.1 ± 0.3 {11}	23.9 ± 20.5$^{2-3}$	4.8 ± 1.5
$11E_b$	0.91 ± 0.50	n.d.	1.05 ± 0.03	0.03 ± 0.02	n.d.	0.14 ± 0.02	20.4 ± 10.6	n.d.	12.3 ± 3.6

Data were treated within "container" model n.d., not determined

Superscripts denote the significant ($P < 0.05$) differences: $^{2-3}$ E23 vs. E33 in-row comparison; $^{2-4}$ E23 vs. E34 in-row comparison; $^{3-4}$ E33 vs. E34 in-row comparison. The single number in curly brackets belongs to a particular peak number at in-column comparison

Table 4 Bivariate analysis for apoE content and parameters of the "container" model for E33 group in the displacement study

Variable 1	Variable 2		
$1E_b$	A_3:$1E_b$ (−0.83)	A_3:$10E_b$ (+0.97)	
$2E_b$	A_2:$2E_b$ (+0.77)		
$3E_b$	A_2:$4E_b$ (−0.80)		
$4E_b$	A_3:$1E_b$ (+0.76)	A_1:$7E_b$ (−0.89)	
$5E_b$	A_2:$5E_b$ (+0.77)	A_3:$1E_b$ (+0.88)	A_3:$10E_b$ (−0.94)
$6E_b$	A_2:$5E_b$ (−0.80)		
$7E_b$	–		
$8E_b$	A_2:$8E_b$ (+0.78)		
$9E_b$	A_3:$11E_b$ (−1.00)	A_1:$9E_b$ (+0.82)	
$10E_b$	A_3:$1E_b$ (−0.95)	A_3:$2E_b$ (−0.88)	A_3:$3E_b$ (+0.84)
$11E_b$	A_3:$2E_b$ (−0.97)	A_3:$8E_b$ (+1.00)	A_3:$10E_b$ (+1.00)

All values were log-transformed before the analysis. The variables are given together with the significant ($P < 0.05$) r values included in brackets

and cluster analysis for E33 and E34 groups. At least for E33 and E34 groups, there seems to be two significantly different types of apoE package: (a) HDL particles with the high electrophoretic mobility ($E3_b$) and (b) $4E_b$ (not included for E34), $5E_b$, $7E_b$, $9E_b$, and $10E_b$. The other lipoproteins possessed intermediate values for the ratio. For lipoprotein pools the ratio was 2.5 higher for HDL compared to IDL/LDL, while being the highest for VLDL particles.

Discussion

Three questions seem to be important: the validity of using (1) ceramide probe and (2) apoE/F to quantify the distribution of lipid and apolipoprotein constituents among CITP fractions; and (3) the phenotype-dependent apoE binding to VLDL particles.

The observed distribution of ceramide probe between HDL, VLDL, and IDL/LDL as 50:10:40 (Table 1) agrees well with the distribution of neutral endogenous glycosphingolipids glucosylceramide, lactosylceramide, trihexosylceramide, and globoside as 40–50:15–25:30–45 [51] and with the data on the binding of exogenous ^{3}H-glucosylceramide to lipoproteins [52]. The absence of selective binding of the probe to particular lipoproteins is important in quantitative assays. Ceramide, in contrast to sphingomyelin, forms the microdomains in both liquid crystalline and gel states of phosphatidylcholine [53]. The distribution of fluorescent analog of ceramide may comply with the existence of specific binding sites on phospholipid lipoprotein surface, the nature of which needs to be determined. Indeed, the good quantitative compliance between ceramide probe binding to HDL and LDL with phospholipid

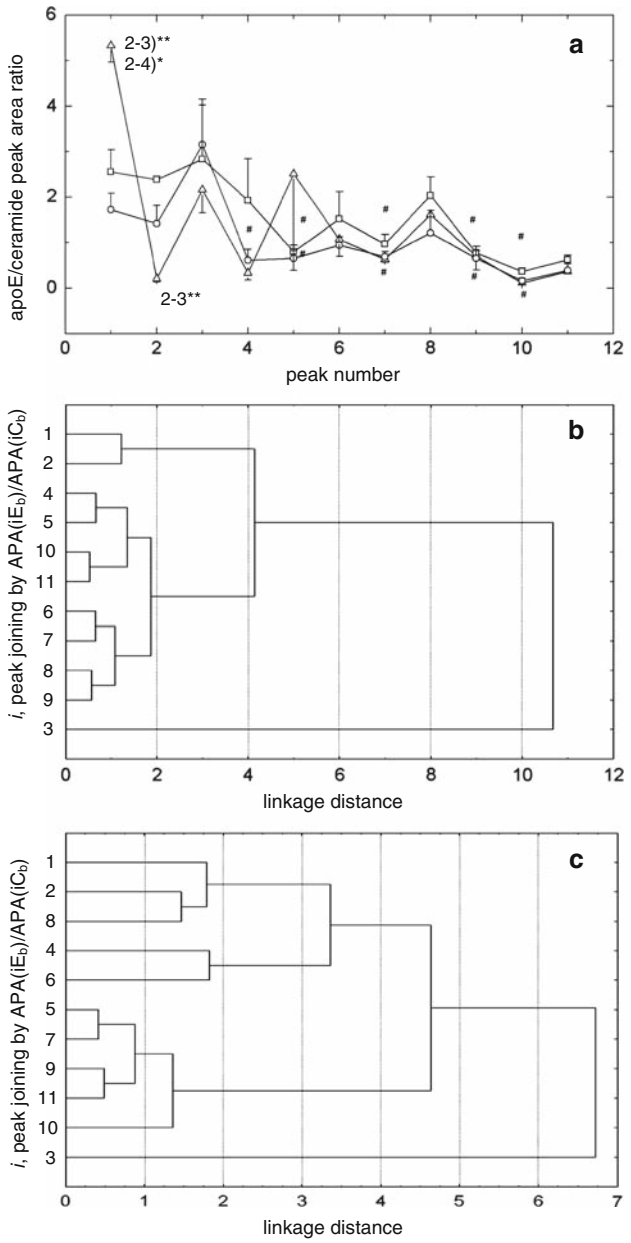

Fig. 4 The relative affinity of apoE in lipoprotein profile. (**a**) group symbols as in Fig. 3, $^{2-3}$ and $^{2-4}$ differ significantly at E23 vs. E33 or E23 vs. E34 at 'between-profile' comparison by *t*-test, $^{\#}$ differ significantly at "in-profile" comparison of a particular peak with $3E_b$; (**b**) tree-clustering analysis for E33 group; (**c**) tree-clustering analysis for E34 group. In cluster analysis, tree diagram for individual peaks as variables was constructed with complete linkage as joining rule and Euclidean distance as distance metric

content was demonstrated earlier [24]. So, the distribution of ceramide probe between individual lipoproteins determined by the phospholipid content in the surface monolayer of spherical lipoproteins or in the bilayer of discoidal HDL particles is assumed in the quantitative assessment of lipoprotein lipid heterogeneity by CITP. Taking into consideration the location of VLDL within $8C_b$ (Fig. 1), the relative position of the particular lipoprotein within the profile (Fig. 2) and our previous findings [24], the general correspondence between lipoprotein fractions by CITP, ultracentrifuge, and agarose gel electrophoresis may be outlined as follows: $1–6C_b$–HDL_2 and HDL_3 particles with α-mobility; $7C_b$–discoidal HDL_2 with preβ-mobility; $8C_b$-VLDL particles with preβ-mobility; $9–12C_b$-IDL/LDL particles with β-mobility.

The principal new finding is the usage of fluorescein-labeled apoE to follow apolipoprotein distribution between lipoproteins and to measure apoE content in $8E_b$ peak with VLDL particles (Fig. 3). The increased ratio of the fluorescence intensities of apoE/F and ceramide probe in the HDL pool compared to that in IDL/LDL pool is explained reasonably well by the increased sphingomyelin content in LDL when compared to HDL, i.e., 14.5 vs 9.2 weight %, respectively [54]. 62–70% of apoE staining originates from HDL region ($1–7E_b$) and 9–19% of the probe molecules localize in VLDL that coincides well with the data on apoE distribution [33].

The next important finding in the present study is the preferential localization of apoE/F in VLDL in E34 heterozygotes compared to E33 homozygotes. The interaction between N- and C-terminal domains only in apoE4 molecule and not in apoE3, suggested by us [10, 15] and others [55] may underlie both the preferential binding of apoE4 to lipoproteins larger than HDL and the absence of contribution from the curvature of lipoprotein surface to apoE3 binding.

It was possible, also, to quantitatively describe the simultaneous apoE binding to all lipoproteins in whole plasma. Data were treated within the "container" model, where the apoE-apoC-III competition for lipoprotein is directed by the size of a particular lipoprotein container rather than plasma apoC-III content applied by others [7]. In the latter case, the interaction of apoC-III with lipoproteins other than that under consideration has been omitted. The existence of a non-zero non-displaceable pool of apoE in VLDL does not coincide with the other data [7], when non-diplaceable apoE was observed only in giant VLDL particle with more than 40,000 triglyceride molecules. This discrepancy may be explained by both the difference in VLDL composition and data treatment. The existence of kinetically heterogeneous pools of apoA-I, apoA-II apoC-III-1 at exchange between small unilamellar vesicles [56] and of apoC-III at exchange between VLDL and HDL_3 [57] also suggests the non-exchanging, within days/week period, pool of these apolipoproteins. The existence of different apolipoprotein conformations on lipoprotein surface may underly this common phenomenon. The apoE content in $9E_b$ directly correlated with A_1 parameter for E33 group. Protein–protein interactions are assumed to control apoE content in this remnant lipoprotein. Indeed, we described earlier [24] apoE clusters on the

VLDL surface with the dimensions growing at the increase of plasma triglyceride. Otherwise, apoE content may be controlled by the relative apoE affinity ($1E_b$) or maximal sorbtion capacity ($2E_b$, $5E_b$, $8E_b$). In a more complex manner, apoE content within $1E_b$, $4E_b$, $5E_b$, $9E_b$, $10E_b$, $11E_b$ seems to be sensitive to apoE binding by other lipoproteins (Table 4) that coincides well with the second type of apoE package within these lipoproteins (Fig. 4).

In conclusion, a CITP-based approach for the measurement of apoE distribution among lipoproteins in whole plasma was developed and the isoform-specific distribution of apoE was observed thus involving a two-domain model of apoE structure in solution to describe apolipoprotein–lipid interaction. This study provides the first insight into the relationships between apoE distribution and apolipoprotein binding parameters. The simultaneous detection of lipid and exchangeable apolipoproteins within all lipoprotein compartments is believed to be a promising approach in lipoproteomics. Indeed, a present approach may be suggested as a method of choice to quickly and effectively monitor various dyslipidemias at prevention, diagnosis, and treatment steps including the search of molecular targets at structural level.

Acknowledgments A.D.D. thanks the Russian Foundation for Basic Research for financial support, grant 07-04-00377.

References

1. Austin MA (2000) Triglyceride, small, dense low-density lipoprotein, and the atherogenic lipoprotein phenotype. Curr Atheroscler Rep 2:200–207. doi:10.1007/s11883-000-0021-4
2. Grundy SM, Mok HY, Zech L et al (1979) Transport of very low density lipoprotein triglycerides in varying degrees of obesity and hypertriglyceridemia. J Clin Invest 63:1274–1283. doi:10.1172/JCI109422
3. Dergunov AD (2004) Apolipoprotein E structure and substrate and receptor-binding activities of triglyceride-rich human plasma lipoproteins in normo- and hypertriglyceridemia. Biochemistry (Mosc) 69:720–737. doi:10.1023/B:BIRY.0000040195.34986.93
4. Dergunov AD, Novoselov AV, Visvikis S et al (2005) The composition, structural properties and binding of very-low-density and low-density lipoproteins to the LDL receptor in normo- and hypertriglyceridemia: relation to the apolipoprotein E phenotype. Biol Chem 386:441–452. doi:10.1515/BC.2005.053
5. Rensen PCN, van Berkel TJC (1996) Apolipoprotein E effectively inhibits lipoprotein lipase-mediated lipolysis of chylomicron-like triglyceride-rich lipid emulsions in vitro and in vivo. J Biol Chem 271:14791–14799. doi:10.1074/jbc.271.25.14791
6. Aalto-Setala K, Weinstock PH, Bisgaier CL et al (1996) Further characterization of the metabolic properties of triglyceride-rich lipoproteins from human and mouse apoC-III transgenic mice. J Lipid Res 37:1802–1811
7. Breyer ED, Le N-A, Li X et al (1999) Apolipoprotein C-III displacement of apolipoprotein E from VLDL: effect of particle size. J Lipid Res 40:1875–1882
8. Chung BH, Dashti N (2000) Lipolytic remnants of human VLDL produced in vitro: effect of HDL levels in the lipolysis mixtures on the apoCs to apoE ratio and metabolic properties of VLDL core remnants. J Lipid Res 41:285–297
9. Hofman A, Ott A, Breteler MM et al (1997) Atherosclerosis, apolipoprotein E, and prevalence of dementia and Alzheimer's disease in the Rotterdam Study. Lancet 349:151–154. doi:10.1016/S0140-6736(96)09328-2
10. Barbier A, Clement-Collin V, Dergunov AD et al (2006) The structure of human apolipoprotein E2, E3 and E4 in solution. 1. Tertiary and quaternary structure. Biophys Chem 119:158–169. doi:10.1016/j.bpc.2005.07.010
11. Dergunov AD, Shuvaev VV, Yanushevskaja EV (1992) Quaternary structure of apolipoprotein E in solution: fluorimetric, chromatographic and immunochemical studies. Biol Chem Hoppe Seyler 373:323–331
12. Dergunov AD, Vorotnikova YY, Visvikis S et al (2003) Homo- and hetero-complexes of exchangeable apolipoproteins in solution and in lipid-bound form. Spectrochim Acta A Mol Biomol Spectrosc 59:1127–1137. doi:10.1016/S1386-1425(02)00298-6
13. Acharya P, Segall ML, Zaiou M et al (2002) Comparison of the stabilities and unfolding pathways of human apolipoprotein E isoforms by differential scanning calorimetry and circular dichroism. Biochim Biophys Acta 1584:9–19
14. Morrow JA, Hatters DM, Lu B et al (2002) Apolipoprotein E4 forms a molten globule. A potential basis for its association with disease. J Biol Chem 277:50380–50385. doi:10.1074/jbc.M204898200
15. Clement-Collin V, Barbier A, Dergunov AD et al (2006) The structure of human apolipoprotein E2, E3 and E4 in solution. 2. Multidomain organization correlates with the stability of apoE structure. Biophys Chem 119:170–185. doi:10.1016/j.bpc.2005.07.009
16. Cohn JS, Tremblay M, Amiot M et al (1996) Plasma concentration of apolipoprotein E in intermediate-sized remnant-like lipoproteins in normolipidemic and hyperlipidemic subjects. Arterioscler Thromb Vasc Biol 16:149–159
17. Gibson JC, Rubinstein A, Bukberg PR et al (1983) Apolipoprotein E-enriched lipoprotein subclasses in normolipidemic subjects. J Lipid Res 24:886–898
18. Hannuksela ML, Brousseau ME, Meyn SM et al (2002) In vivo metabolism of apolipoprotein E within the HDL subpopulations LpE, LpE:A-I, LpE:A-II and LpE:A-I:A-II. Atherosclerosis 165:205–220. doi:10.1016/S0021-9150(02)00200-9
19. Huang Y, von Eckardstein A, Wu S et al (1994) A plasma lipoprotein containing only apolipoprotein E and with γ mobility on electrophoresis releases cholesterol from cells. Proc Natl Acad Sci USA 91:1834–1838. doi:10.1073/pnas.91.5.1834
20. Krimbou L, Tremblay M, Davignon J et al (1997) Characterization of human plasma apolipoprotein E-containing lipoproteins in the high-density lipoprotein size range: focus on pre-β1-LpE, pre-β2-LpE, and α-LpE. J Lipid Res 38:35–48
21. Krimbou L, Marcil M, Chiba H et al (2003) Structural and functional properties of human plasma high density-sized lipoprotein containing only apoE particles. J Lipid Res 44:884–892. doi:10.1194/jlr.M200273-JLR200
22. Bittolo-Bon G, Cazzolato G (1999) Analytical capillary isotachophoresis of total plasma lipoproteins: a new tool to identify atherogenic low density lipoproteins. J Lipid Res 40:170–177
23. Bottcher A, Schlosser J, Kronenberg F et al (2000) Preparative free-solution isotachophoresis for separation of human plasma lipoproteins: apolipoprotein and lipid composition of HDL subfractions. J Lipid Res 41:905–915
24. Dergunov AD, Hoy A, Smirnova EA et al (2003) Charge-based heterogeneity of human plasma lipoproteins at hypertriglyceridemia: capillary isotachophoresis study. Int J Biochem Cell Biol 35:530–543. doi:10.1016/S1357-2725(02)00359-X
25. Schlenck A, Herbeth B, Siest G et al (1999) Characterization and quantification of serum lipoprotein subfractions by capillary

isotachophoresis: relationships with lipid, apolipoprotein, and lipoprotein levels. J Lipid Res 40:2125–2133
26. Zhang B, Miura S, Fan P et al (2005) ApoA-I/phosphatidylcholine discs remodels fast-migrating HDL into slow-migrating HDL as characterized by capillary isotachophoresis. Atherosclerosis 188:95–101. doi:10.1016/j.atherosclerosis.2005.10.032
27. Zorn U, Wolf CF, Wennauer R et al (1999) Separation of lipoproteins by capillary isotachophoresis combined with enzymatic derivatization of cholesterol and triglycerides. Electrophoresis 20:1619–1626 doi:10.1002/(SICI)1522-2683(19990601)20:7<1619::AID-ELPS1619>3.0.CO;2-U
28. Soderlund S, Soro-Paavonen A, Ehnholm C et al (2005) Hypertriglyceridemia is associated with preβ-HDL levels in subjects with familial low HDL. J Lipid Res 46:1643–1651. doi:10.1194/jlr.M400480-JLR200
29. Kypreos KE, van Dijk KW, Havekes LM et al (2005) Generation of a recombinant apolipoprotein E variant with improved biological functions. Hydrophobic residues (LEU-261, TRP-264, PHE-265, LEU-268, VAL-269) of apoE can account for the apoE-induced hypertriglyceridemia. J Biol Chem 280:6276–6284. doi:10.1074/jbc.M413458200
30. Tomiyasu K, Walsh BW, Ikewaki K et al (2001) Differential metabolism of human VLDL according to content of apoE and apoC-III. Arterioscler Thromb Vasc Biol 21:1494–1500. doi:10.1161/hq0901.094489
31. Dallongeville J, Bauge E, Lebel P et al (1997) Fat ingestion is associated with increased levels of apoC-III- and apoE-B-containing lipoprotein particles in humans. Eur J Clin Invest 27:1055–1060. doi:10.1046/j.1365-2362.1997.2350782.x
32. Fredenrich A, Giroux LM, Tremblay M et al (1997) Plasma lipoprotein distribution of apoC-III in normolipidemic and hypertriglyceridemic subjects: comparison of the apoC-III to apoE ratio in different lipoprotein fractions. J Lipid Res 38:1421–1432
33. Rubinstein A, Gibson JC, Paterniti JR Jr et al (1985) Effect of heparin-induced lipolysis on the distribution of apolipoprotein E among lipoprotein subclasses. Studies with patients deficient in hepatic triglyceride lipase and lipoprotein lipase. J Clin Invest 75:710–721. doi:10.1172/JCI111751
34. Tam SP, Dory L, Rubinstein D (1981) Fate of apolipoproteins C–I, C-III, and E during lipolysis of human very low density lipoproteins in vitro. J Lipid Res 22:641–651
35. Chiba H, Akizawa K, Fujisawa S et al (1992) A rapid and simple quantification of human apolipoprotein E-rich high-density lipoproteins in serum. Biochem Med Metab Biol 47:31–37. doi:10.1016/0885-4505(92)90005-J
36. Cohn JS, Marcoux C, Davignon J (1999) Detection, quantification, and characterization of potentially atherogenic triglyceride-rich remnant lipoproteins. Arterioscler Thromb Vasc Biol 19:2474–2486
37. Connelly PW, Maguire GF, Vezina C et al (1994) Kinetics of lipolysis of very low density lipoproteins by lipoprotein lipase. Importance of particle number and noncompetitive inhibition by particles with low triglyceride content. J Biol Chem 269:20554–20560
38. de Man FHAF, de Beer F, van der Laarse A et al (2000) The hypolipidemic action of bezafibrate therapy in hypertriglyceridemia is mediated by upregulation of lipoprotein lipase: no effects on VLDL substrate affinity to lipolysis or LDL receptor binding. Atherosclerosis 153:363–371. doi:10.1016/S0021-9150(00)00409-3
39. Quinn DM, Shirai K, Jackson RL et al (1982) Lipoprotein lipase catalyzed hydrolysis of water-soluble p-nitrophenyl esters. Inhibition by apolipoprotein C-II. Biochemistry 21:6872–6879. doi:10.1021/bi00269a038
40. Jonas A (1998) Regulation of lecithin cholesterol acyltransferase activity. Prog Lipid Res 37:209–234. doi:10.1016/S0163-7827(98)00007-1
41. Havel RJ, Eders HA, Bragdon JH (1955) The distribution and chemical composition of ultracentrifugally separated lipoproteins in human serum. J Clin Invest 34:1345–1353. doi:10.1172/JCI103182
42. Dergunov AD, Aniskovich LP, Shuvaev VV (1990) Affinity chromatography on heparin-sepharose under reducing conditions as a method of selective enrichment with individual isoforms of apolipoprotein E. Bull Exp Biol Med 110:894–898. doi:10.1007/BF00839921
43. Dergunov AD, Shuvaev VV, Sokol'nikov AA et al (1985) Kinetics of the hydrolysis of triolein by lipoprotein lipase in the presence of apoprotein C-II. Proc Acad Sci USSR 281:39–43
44. Fontana A, Gross E (1986) Fragmentation of polypeptides by chemical methods. In: Darbre A (ed) Practical protein chemistry: a handbook. Wiley, Chichester, UK, pp 67–120
45. Bradford MM (1976) A rapid and sensitive method for the quantitation of microgram quantities of protein utilizing the principle of protein-dye binding. Anal Biochem 72:248–254. doi:10.1016/0003-2697(76)90527-3
46. Borochov-Neori H, Montal M (1983) Rhodopsin in reconstituted phospholipid vesicles. 1. Structural parameters and light-induced conformational changes detected by resonance energy transfer and fluorescence quenching. Biochemistry 22:197–205. doi:10.1021/bi00270a029
47. Schmitz G, Mollers C, Richter V (1997) Analytical capillary isotachophoresis of human serum lipoproteins. Electrophoresis 18:1807–1813. doi:10.1002/elps.1150181015
48. Assmann G, Schriewer H, Schmitz G et al (1983) Quantification of high-density lipoprotein cholesterol by precipitation with phosphotungstic acid/$MgCl_2$. Clin Chem 29:2026–2030
49. Friedewald WT, Levy RI, Fredrickson DS (1972) Estimation of the concentration of low-density lipoprotein cholesterol in plasma, without use of the preparative ultracentrifuge. Clin Chem 18:499–502
50. Hixson JE, Vernier DT (1990) Restriction isotyping of human apolipoprotein E by gene amplification and cleavage with Hha I. J Lipid Res 31:545–548
51. van den Bergh FA, Tager JM (1976) Localization of neutral glycosphingolipids in human plasma. Biochim Biophys Acta 441:391–402
52. Clarke JT, Stoltz JM (1976) Uptake of radiolabeled galactosyl-(alpha1 goes to 4)-galactosyl-(beta1 goes to 4)-glucosylceramide by human serum lipoproteins in vitro. Biochim Biophys Acta 441:165–169
53. Holopainen JM, Lemmich J, Richter F et al (2000) Dimyristoylphosphatidylcholine/C16:0-ceramide binary liposomes studied by differential scanning calorimetry and wide- and small-angle x-ray scattering. Biophys J 78:2459–2469
54. Skipski VP, Barclay M, Barclay RK et al (1967) Lipid composition of human serum lipoproteins. Biochem J 104:340–352
55. Dong LM, Weisgraber KH (1996) Human apolipoprotein E4 domain interaction. Arginine 61 and glutamic acid 255 interact to direct the preference for very low density lipoproteins. J Biol Chem 271:19053–19057. doi:10.1074/jbc.271.32.19053
56. Ibdah JA, Smith C, Lund-Katz S et al (1991) Effects of apolipoprotein structure on the kinetics of apolipoprotein transfer between phospholipid vesicles. Biochim Biophys Acta 1081:220–228
57. Boyle KE, Phillips MC, Lund-Katz S (1999) Kinetics and mechanism of exchange of apolipoprotein C-III molecules from very low density lipoprotein particles. Biochim Biophys Acta 1430:302–312